Influence of Gamma Energy in the Image Contrast for Material with Different Density

Article · May 2010

CITATIONS
0

READS
16

3 authors, including:

Reza Gholipour-Peyvandi
Nuclear Science and Technology Research, Iran
37 PUBLICATIONS **38** CITATIONS
SEE PROFILE

Seyedeh Zahra Islami rad
Amirkabir University of Technology
26 PUBLICATIONS **9** CITATIONS
SEE PROFILE

International Journal of Pure and Applied Physics
ISSN 0973-1776 Volume 6, Number 4 (2010), pp. 447–454

http://www.ripublication.com/ijpap.htm

Influence of Gamma Energy in the Image Contrast for Material with Different Density

R. Gholipour-Peyvandi, S.Z. Islami-Rad* and M. Ghannadi-Maragheh

Nuclear science and technology research institute,
end of north Kargar, Tehran – Iran
**Ccorresponding Author E-mail: szislami@yahoo.com*

Abstract

Different technical and physical factors may influence the image quality. For studying the effect of some important factors an industrial computed tomography (CT) system was designed and developed on the base of the first generation CT system. The CT scanner consists of a 5.08cm NaI(Tl) detector, and a source collimator 5mm in width. In this study, we have investigated the effects of energy, density and counting time on reconstructed image quality experimentally. For this reason, several experiments were performed using ^{75}Se (264 keV-58.9%, 279 keV-24.9%), ^{137}Cs (662 keV), ^{60}Co (1332 keV) sources and with different of energy. The energy windows for applied sources are ^{137}Cs (662±90 keV), ^{60}Co (1332 keV±90 keV) and ^{75}Se (270± 80 keV), respectively. Also, for studying of density, a polyethylene phantom (9.3E-01g.cm^{-3}) was used. The phantom was made as cylindrical geometry on which 3 holes of 15 mm in diameter were improvised. The holes were filled with mercury (1.353E+01g·cm^{-3}), iron (7.874g·cm^{-3}), air (1.184E-03g·cm^{-3}) and scans were performed in counting time 15s and 25 s. Finally, the quality of different images is analyzed by computing the RMS contrast of each image to compare materials with least density and the greatest density.

Keywords: Industrial CT, design and development, energy of sources, different density, counting time, filtered back- projection, contrast.

Introduction

Nuclear imaging systems, such as gamma computed tomography, are able to analyze and identify failures in industrial processes, permitting to visualize failure points [1,2].

Computed tomography is a noninvasive imaging technique that has been used extensively not only in medicine diagnosis and surgical planning, but also in nondestructive testing (NDT) for many industrial applications such as mechanical part manufacturing, production of composite materials, waste container inspection, metrology, detection of structural defects and others, heterogeneities in polymer objects, etc [3- 6].

The goal of industrial gamma ray CT is to produce internal images of object with sufficient detail to detect important features. The visibility of an image depends on the difference in gamma rays attenuation between the features and its back ground. This valuable characteristic is contrast. Contrast is usually used to assess the performance of a gamma ray CT [7].

In gamma ray CT, the contrast is affected by several factors. These factors are detector, collimator, counting time, etc [8-10]. In this study, we considered several factors that mainly influence the contrast. In order to study the effect of energy factor, three sources with different energy were studied. The other factors are counting time and the density of materials (mercury, air and iron). The results of root mean square (RMS) contrast demonstrated the effect of above factors on reconstructed image contrast.

Theory

Main parts of CT scanner include of a γ-ray source, a platform that holds the object, and a detector [11].

Tomography imaging consists of directing γ-rays onto an object from multiple orientations and measuring the decrease in intensity along a series of linear paths. This decrease is characterized by Beer's Law, which describes intensity reduction as a function of γ-ray energy, path length, and linear attenuation coefficient of material. A specialized algorithm is then used to reconstruct the distribution of γ-ray attenuation in the volume being imaged [11].

In the reconstructed image, contrast is a valuable characteristic. Contrast is the difference in visual properties that makes an object (or its representation in an image) distinguishable from other objects and the background. There are some definites for calculating contrast. In this paper, RMS contrast was used.

RMS contrast

RMS contrast does not depend on the spatial frequency content or the spatial distribution of contrast in the image. RMS contrast is defined as the standard deviation of the pixel intensities.

$$RMS\ contrast = \sqrt{\frac{1}{MN}\sum_{i=0}^{N-1}\sum_{j=0}^{M-1}(I_{ij}-\bar{I})^2} \quad (1)$$

where intensities I_{ij} are the i-th and j-th elements of the two dimensional image of size M by N. $\bar{I}$ is the average intensity of all pixel values in the image[12]. The image I is assumed to have its pixel intensities normalized in the range (0,1).

Effects of energy on contrast for different density

In a gamma-ray transmission, I, of a mono-energetic radiation beam traversing a phantom of thickness is given by the following equation:

$$I = I_0 e^{-\int \mu(i,j)\, du} \quad (2)$$

Where I_0 is the incident beam intensity of the radiation beam, du is some different path length and μ (i, j) is the function describing the 2 dimensional distribution of attenuation coefficient in the imaged object [13].

Attenuation coefficient changes with effects of Raleigh, photoelectric, Compton and pair product. $\mu_{photoelectric}$ has a great dependence on the atomic number of the absorber, a primary reason for more attenuation which reduces by increasing incident photon energy (Eγ). Also, $\mu_{Compton}$ is almost independent of atomic number (Z)[13]. Thus, incident photon energy plays an important role in attenuation coefficient. Also, the total attenuation coefficient increases as atomic number (Z) and density increase (Fig.1) [14].

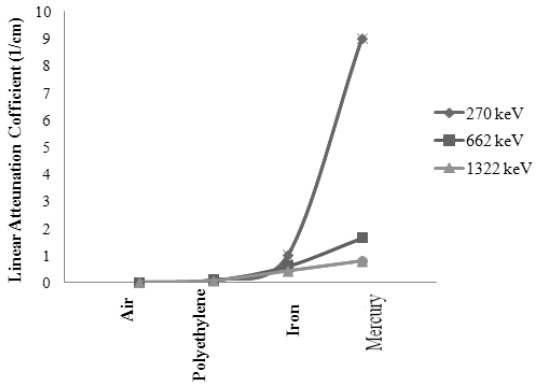

Figure 1: Attenuation coefficient (μ) vs. material.

As a result, contrast increases when total attenuation coefficient increases.

Also, it is obvious that counts increase when the sampling time in each projection increases and the relative noise decreases. The noise depending on the number of detected particles section is almost independent of atomic number (Z). As a result, increasing of counting time improves the contrast [15].

Materials and methods

A single-source – single-detector gamma computed tomography (CT) scanner system was used in this study. This system consists of a NaI(Tl) detector 5.08 cm in diameter

(2×2, 905-3 model, ORTEC company). Also, three different encapsulated radioactive sources as ^{75}Se (40 mCi), ^{137}Cs (30 mCi) and ^{60}Co (10 mCi) were used in this study, separately. The detector and the source were placed on a fixed support and the phantom could be rotated between them. The detector and the source were aligned by a point semiconductor laser.

A polyethylene phantom (9.3E- 01g.cm^{-3}) was used to determine the 2D imaging quality of the designed industrial CT system. The phantom was made as cylindrical geometry on which 3 holes of 15 mm in diameter were improvised. The holes were filled with mercury (1.353E+01g·cm^{-3}), iron (7.874g·cm^{-3}), air (1.184E-03g·cm^{-3}) (Fig. 2).

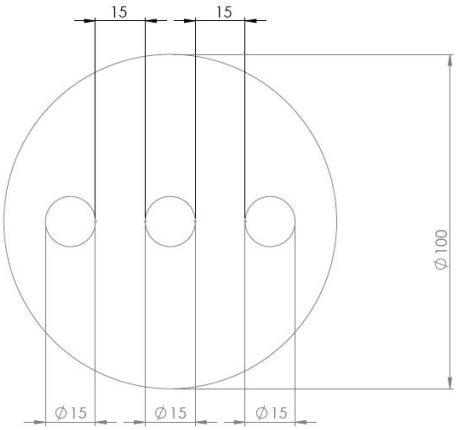

Figure 2: Polyethylene phantom of 3 holes (15 mm), phantom diameter: 10 cm.

Two cylindrical lead collimators were used for source and detector. Also, the source - detector distance was 55cm. In this system, phantom had 3 dimensional rotation capability using controller motors in the cylindrical coordinate (R, θ,Z). R & Z motors were shifted with 0.01^{o} step and the θ motor had 360^{o} rotation potential with 0.04^{o}step and more. Three motors set the defined position of the phantom. A schematic design of the system hardware was shown in Fig. 3.

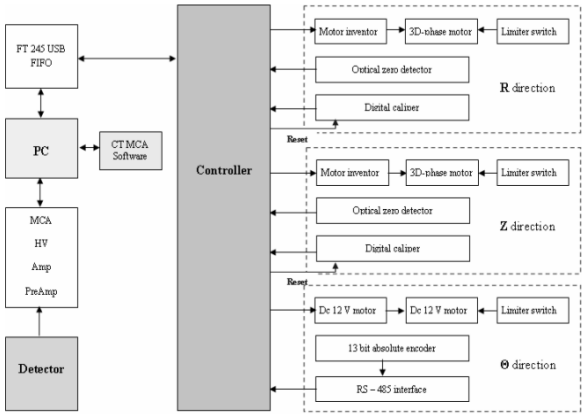

Figure 3: Computed tomography system hardware diagram.

In each movement, the phantom rotated by 4^{o}. Also, the CT scans were taken by scanning 180^{o} to collect attenuation beams. A set of independent projections for the same step was recorded by rotating phantom and the attenuated radiation were measured by a detector.

Nuclear electronic system consists of a NaI(Tl) (2×2, 905-3 model, ORTEC company), and a specialized MCA (PSS-1, NSTRI, Tehran, Iran) consists of pre-amplifier, amplifier, high voltage (HV) and a data acquisition system. In this MCA, universal written software can simultaneously read positions and steps, control the motors and MCA. After that, the image is reconstructed from the measured projections by the filtered back projection method to perform the inverse Radon transform.

Results

The results are represented using reconstructed images consisting of the RMS contrast.

In this research, experimental conditions for improving contrast such as energy, density and counting time were tested in different study cases (Fig. 4). The fisrt case (1) represents the results with a source of ^{75}Se (270 keV), a collimator (5mm diameter), a phantom with 3 holes and a counting time 15 s. The second case (2) represents a sources of ^{137}Cs (662 keV), a collimator (5mm diameter), a phantom with 3 holes and a counting time 15 s. The third case (3) represents a source of ^{60}Co (1332 keV), a collimator (5mm diameter), a phantom with 3 holes and a counting time 15 s. The fourth case (4) represents a sources of ^{75}Se (270 keV), a collimator (5mm diameter), a phantom with 3 holes and a counting time 25 s. The fifth case (5) represents a source of ^{137}Cs (662 keV), a collimator (5mm diameter), a phantom with 3 holes and a counting time 25 s. The Sixth case (6) represents a source of ^{60}Co (1332 keV), a collimator (5mm diameter), a phantom with 3 holes and a counting time 25 s. The RMS contrast of each material was given for different energy, density and counting time (Table 1& 2). Also, the RMS contrast of entire phantom was given for different energy and counting time (Table 3).

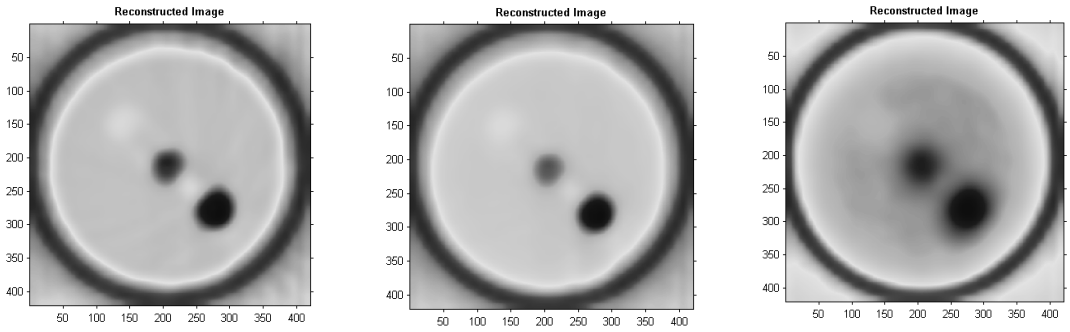

1 2 3

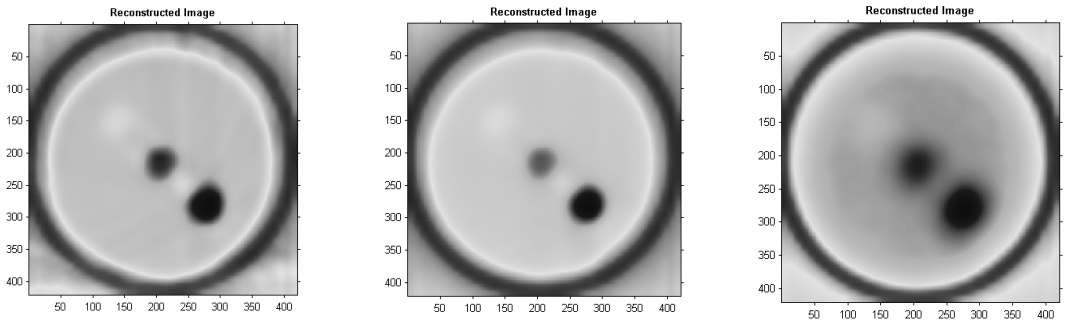

Figure 4: Polyethylene phantom 2D image, mercury, iron, air holes for different energy and density.

Table 1: RMS contrast in counting time: 15 second.

Source	^{75}Se			^{137}Cs			^{60}Co		
Material	Air	Iron	Mercury	Air	Iron	Mercury	Air	Iron	Mercury
RMS Contrast	146.10	450.91	637.46	59.61	195.41	355.96	14.98	41.29	65.46

Table 2: RMS contrast in counting time: 25 second.

Source	^{75}Se			^{137}Cs			^{60}Co		
Material	Air	Iron	Mercury	Air	Iron	Mercury	Air	Iron	Mercury
RMS Contrast	241.66	562.16	872.90	94.91	280.81	477.22	22.79	66.98	107.02

Table 3: RMS contrast for entire phantom.

Source	^{75}Se	^{137}Cs	^{60}Co
RMS Contrast (15 s)	475.98	257.69	84.19
RMS Contrast (25 s)	630.03	307.14	93.77

Discussion

It can be observed that RMS contrast for ^{60}Co with higher energy is less than that of ^{137}Cs. RMS contrast of ^{75}Se with lower energy is better than ^{137}Cs (Fig. 4, Table 3). In the phantom with different materials, RMS contrast for mercury is the highest (Fig. 5).

Also, is observed that RMS contrast in counting time of 25 s is better than counting time of 15 s and increasing of counting time at lower energy levels has a stronger effect on contrast improvement (Fig. 6).

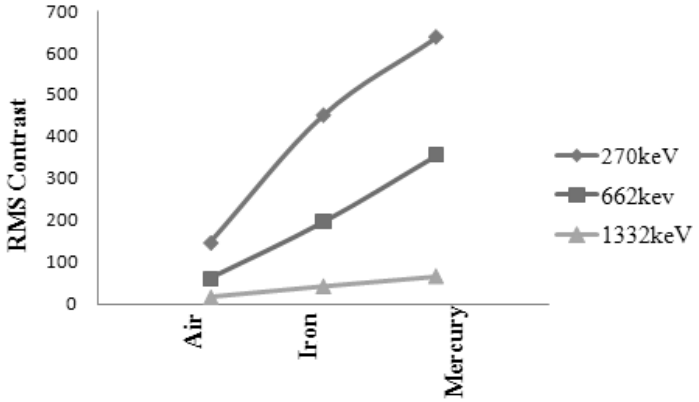

Figure 5: RMS contrast as a function of material.

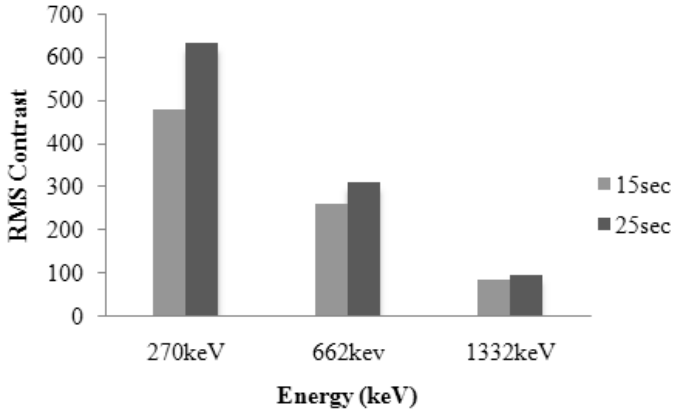

Figure 6: RMS contrast as a function of counting time.

Conclusion

The phantom consists of four different materials with an extensive range of densities and by comparing different sources, the results demonstrate the contrast is depended on atomic number (Z) and the extent of densities in additional energy. Also, contrast is better in lower energy. Thus, for improving quality image should select materials with high density or extensive range of densities and low energy source.

References

[1] Noel, J., 2008, "Advantages of CT in 3D Scanning of Industrial Parts," North Star Imag Inc. J., 1, pp. 18.

[2] de Oliveira Jr, J.M., Martins, A.C.G., DE Milito, J.A., 2004, " Analysis of Concrete Material through Gamma Ray Computerized Tomography," Braz. J. Phys., 34 (3A), pp. 1020-1022.

[3] Calvo, W.A.P., Hamada, M.M., Sprenger, F.E et al., 2009, "Gamma-ray Computed Tomography SCANNERS for Applications in Multiphase System Columns," NUKLEONIKA., 54 (2), pp.129-133.

[4] Camp, D.C., Martz, H.E., Roberson, G.P., Decman, D.J., Bernardi, R.T., 2002, "Nondestructive Waste-Drum Assay for Transuranic Content by Gamma-Ray Active and Passive Computed Tomography," Nucl. Instrum. Meth A., 495(1), pp. 69-83.

[5] Lettenbauer, H., Georgi, B., Weiß, D., 2007, "Means to Verify the Accuracy of CT Systems for Metrology Applications," DIR 2007 - International Symposium on Digital industrial Radiology and Computed Tomography, Lyon, France.

[6] Braz, D., Lopes, R.T., da Motta, L.M.G., 2000, "Computed Tomography: an Evaluation of the Effect of Adding Polymer SBS to Asphaltic Mixtures Used in Paving," Appl. Radiat. Isotopes., 53(4-5), pp. 725-729.

[7] IAEA-TECDOC 1589., 2008, "Industrial process gamma tomography, final report of a coordinated research project 2003-2007," International Atomic Energy Agency. Austria.

[8] Wu, Z.H., Liu, J., 2009, "Experimental Research on Rear Collimator in ϒ- Ray Industrial CT," Apppl. Radiat. Isotopes., 67(7-8), pp. 1216- 1219.

[9] Vasquez, P.A.S., de Mesquita, C.H., Hamada, M., 2007, "Phantom Study Using a First Generation Gamma Tomography System," International Nuclear Atlantic Conference- INAC 2007, Santos, Brazil.

[10] Melcher, C.L., 2005, "Perspectives on the future Development of New Scintillators," Nucl. Instrum. Meth., 537(1-2), pp. 6-14.

[11] Kim, J., Jung, S., Kim, J., 2006, "A Study on Industrial Gamma Ray CT with a Single Source-Detector Pair," Nucl. Engin. Tech., 38 (4), pp. 383-390.

[12] Peli, E., 1990, "Contrast in complex images," Optic Society of America., 7, pp.2032.

[13] Herman, G.T., 1980, "Image Reconstruction from Projections," ed. 1, Academic Press, London.

[14] (Online) Available: http://physics.nist.gov/xaamdi (2010, March 1). National Institute of Standards and Technology, Gaithersburg, MD.

[15] Hilts, M., Duzenli, C., 2004 "Image noise in X-ray CT polymer gel dosimetry," J. of Phy: Conf. Ser. 3, pp. 252–256.